AN INVESTIGATION INTO THE CONVERSION OF METHANOL TO HYDROCARBONS OVER A SAPO-34 CATALYST USING MAGIC-ANGLE-SPINNING NMR AND GAS CHROMATOGRAPHY

Yan XU [a], Clare P. GREY [b], John M. THOMAS [a] and Anthony K. CHEETHAM [a,b]

[a] *Davy Faraday Research Laboratory, The Royal Institution of Great Britain, 21 Albemarle Street, London, W1X 4BS, England*

[b] *The Chemical Crystallography Laboratory, Oxford University, 9 Parks Road, OX1 3PD, England*

Received 9 November 1989; accepted 31 December 1989

^{13}C magic-angle-spinning (MAS) NMR, along with the results of Fourier transform infrared and gas chromatographic analysis, has been used to identify the hydrocarbon products, and to distinguish mobile from static species, formed from methanol within the pores of a H-SAPO-34 catalyst. The reasons for the differences in product distribution within the pores (monitored by MAS NMR) and in the gas phase (monitored chromatographically) are discussed.

1. Introduction

Methanol conversion reactions are valuable industrial processes and have been the focus of much recent research into the development of new catalysts and the elucidation of the relevant reaction pathways [1–3]. The need to minimize liquid products and maximize olefin yield has lead to a new area of scientific research [4], and silicon-aluminium-phosphate based catalysts are particularly attractive in this context. In particular, the smallpore zeolite H-SAPO-34 has proved a good selective catalyst in the methanol conversion process, one recent report indicating yields of greater than 95 percent for the formation of light olefins [5]. Here we report upon the use of ^{13}C NMR to follow the broad course of methanol conversion. Depending upon whether magic-angle spinning is [6,8], or is not [3] employed, the production of both static and mobile product species may be readily monitored in an in-situ sense. In the present work, we compare the product distributions obtained in a static system (by nmr) and a constant flow reactor system.

2. Experimental

SAPO-34 was synthesized hydrothermally at 200 °C using triethylamine as a template, as described previously [9]. X-ray powder diffraction at this stage

confirmed the formation of crystalline, monophasic SAPO-34. The organic template was then removed by calcining at 500–550 °C in air for 3 hours and the product converted to the ammonium form by repeating ion-exchange with a 0.05 M NH_4NO_3 solution at 80 °C three times. The H-form was obtained by deammoniating at 400 °C in vacuo overnight.

Approximately 50 mg of H-SAPO-34 were placed in a Pyrex glass tube which was based on Carpenter's design [7]. Its constriction was sealed off leaving a capsule of suitable dimensions to fit inside a double-bearing zirconia rotor. The sample was dehydrated at 350 °C for 4 hours under vacuum, and then exposed to 33 percent ^{13}C-enriched methanol (e-MeOH) at a pressure of 50 Torr at room temperature. The adsorption was allowed to equilibrate for 2 hours. It was then pumped down, thereby removing most of the physisorbed e-MeOH, and sealed. The sealed cell was heated at different temperatures for various periods of time and subsequently quenched in liquid nitrogen. The samples heated above 400 °C were quenched only in iced water.

M.A.S. N.M.R. spectra were collected at room temperature on a Bruker MSL 200 spectrometer resonating at 50.32 MHZ for ^{13}C. The pyrex capsule was packed in a 7 mm zirconia rotor, using KBr to keep the capsule in place while spinning. Spinning speeds of typically 1.7 kHz were achieved using a double-bearing probe. Depending on the signal and the information required spectra were accumulated with or without proton decoupling and cross-polarisation. Spectra were all referenced using adamantane as an external standard, taking the upfield methine resonance to be 29.23 ppm [10].

Catalytic tests were performed in a flow reactor with reaction temperature of 300 to 450 °C. Catalyst pellets (40 to 60 mesh, 0.1 g) were used with methanol/water feeds of 30/70 to 40/60 (wt percent). The reactant mixture was carried by nitrogen (flow rate 25 ml/min). A weight hour's space velocity (WHSV) of 3 h^{-1} was used and the products were detected gas chromatographically. Experiments were repeated under the same experimental conditions using a pure methanol feed.

In-situ FT-IR experiments were carried out in an environmental DRIFT (Diffuse reflectance infrared Fourier transform) cell [11], with the sample in the centre of a small furnace in the I.R. beam. H-SAPO-34 was activated at 350 °C in the DRIFT cell and catalysis was then performed in-situ, using N_2 (25 ml) as the carrier gas for methanol between room temperature and 450 °C. The I.R. spectra were recorded using a Perkin Elmer 1725X FT-IR spectrometer which has a resolution of 4 cm^{-1} in the 4000 to 400 cm^{-1} range; 400 scans were accumulated for each spectrum.

3. Results and discussion

The ^{13}C MAS NMR spectrum of e-MeOH, adsorbed on H-SAPO-34 and sealed in a glass capsule, contains one resonance at 50 ppm (fig. 1a). On heating

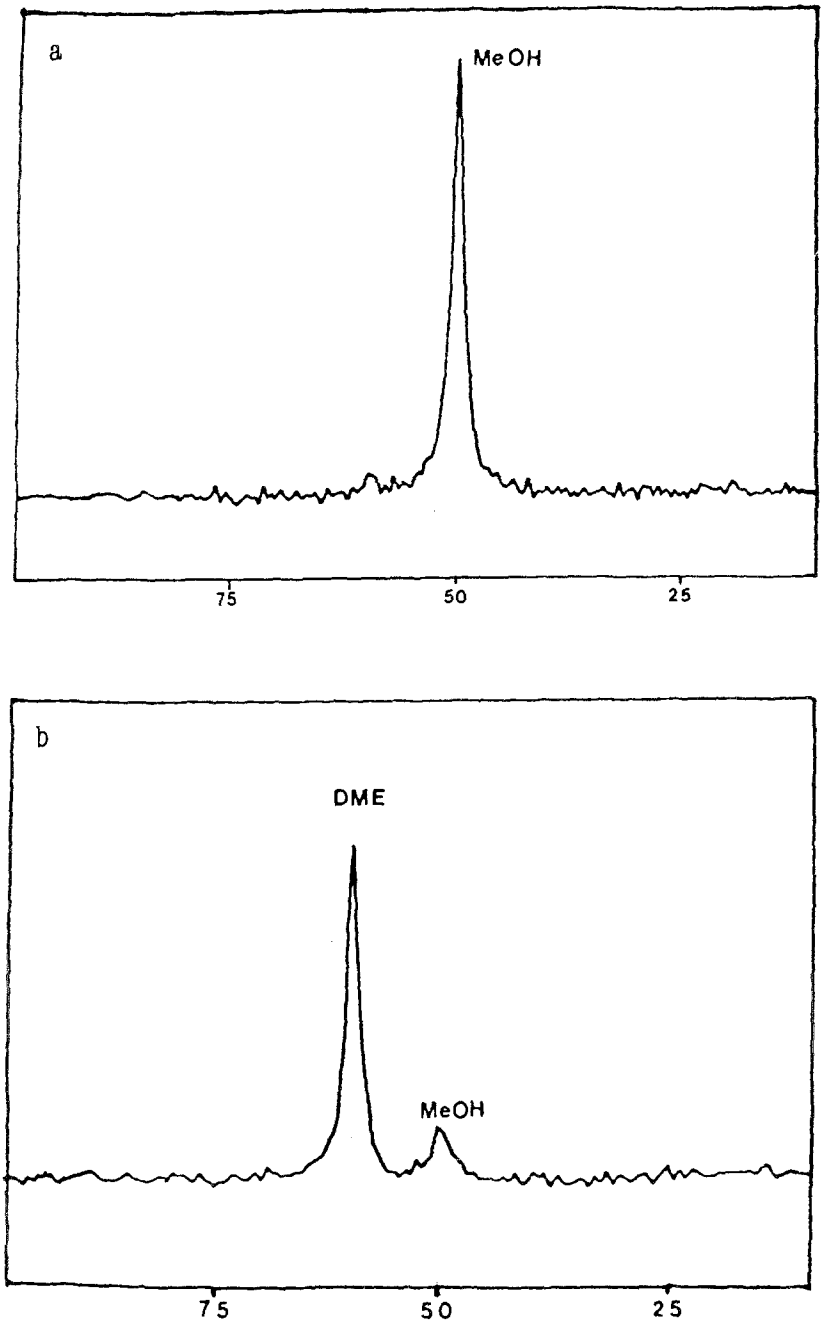

Fig. 1. ^{13}C MAS NMR spectra of enriched methanol adsorbed on a H-SAPO-34 sample. (with proton decouping) a. no heat-treatment applied; b. treated at 250 ° C for 55 min.

at 200 ° C for 10 min a spectrum with two signals, at 50 ppm and 60 ppm, was obtained. These signals correspond to methanol and dimethyl ether (DME) respectively. On treating the same sample at 250 ° C for 55 min., almost total

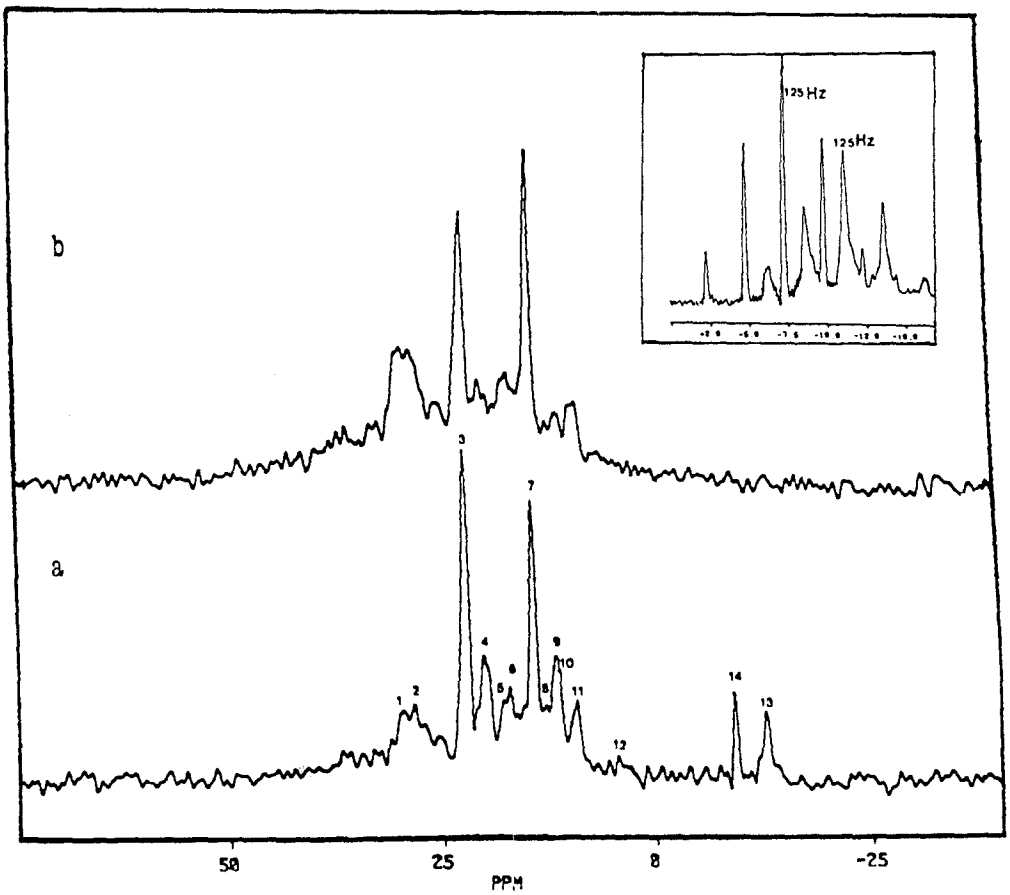

Fig. 2. ^{13}C MAS NMR spectra as observed during the static conversion of methanol on H-SAPO-34 catalyst at 300 °C for 20 min. a. spectrum acquired using proton decoupling; b. spectrum recorded with cross-polarisation. s: strong, m: medium, w: weak, vw: very weak. Methane (12, 13 m); ethane (12, vw); propane (7, 8, s); butanes (3, 9, s); pentanes (1, 2, 4, 9, 10, w); and a very little C-6s. The inset spectrum was recorded without proton decoupling.

conversion to DME is achieved (fig. 1b). At 300 °C resonances in the paraffin region start to appear, the two at 16 and 24 ppm, corresponding to propane and *iso*-butane, being the first products visible. After heating the sample for 20 min (fig. 2) no alcohol or DME remains and there are no signs of any unsaturated hydrocarbons at this stage. In the spectrum collected using cross-polarisation (CP) (fig. 2b), the peaks that were assigned to methane, at −7 and −11 ppm have vanished and those corresponding to the higher hydrocarbons have increased in intensity relative to those in fig. 2a, consistent with their ostensibly reduced mobility in comparison to the lighter hydrocarbons inside the zeolitic structure. On acquiring the spectra without proton decoupling (or CP) the peaks at −7 and −11 ppm could be seen to split up into 2 quintets, both with splittings

of 125 Hz, and intensity ratios of approximately 1 : 4 : 6 : 4 : 1 (shown as the inset in fig. 2). These two peaks can therefore be assigned to methane in two different chemical environments, in which the methane molecule must be sufficiently mobile to average the C-H dipolar coupling to zero, so that no resonances are visible on cross-polarisation. This assignment was further confirmed by adsorbing 100 percent ^{13}C enriched CH_4 onto H-SAPO-34 using the same procedure as used for e-MeOH. The ^{13}C proton decoupled spectrum of this sample also gave two resonances at -7 and -11 ppm.

After further treatment of the sample at 350 °C for 20 min. no significant changes were observed in the aliphatic region of the spectrum. However, resonances at 124.5 ppm and 178 ppm, which were assigned to carbon dioxide and carbon monoxide respectively, started to appear. These assignments are further confirmed by acquiring the spectrum without proton decoupling under which condition the resonances show no splitting. Aromatics are first formed at 400 °C; benzene (128 ppm) and methyl benzenes (134–137 and 125–128 ppm) are clearly visible after heating at 400 °C for 20 min. Heating at 450 °C for 20 min results in increased concentrations of aromatics (shown as the inset in fig. 3), but also the appearance of ethane (5.6 ppm). The amount of ethane tends to remain constant with time. Significantly, the concentration of alkanes with four or more carbons diminishes considerably with time. A quartet centred around 5.6 ppm with a splitting of 120 Hz confirms that this resonance results from adsorbed ethane. After heating at these higher temperatures, the sample darkens, signifying the occurrence of a carbonaceous deposit.

Table 1 lists the various products at different temperatures in the flow reaction system measured by gas chromatography as well as the results from ^{13}C MAS NMR experiments. There are clear differences in product distribution: the former shows mainly alkenes, while the latter indicates only alkanes and aromatics at elevated temperatures. The amount of methane detected by NMR does not decrease drastically as the larger alkanes appear. In neither reactions was there any significant amount of hydrocarbons larger than C_6. It is also noteworthy that the ratio of olefins to paraffins in the flow reaction system varies with the rate of methanol feed and also the ratio of methanol to water. It reaches its maximum for a certain range in flow rate (WHSV from 2 h^{-1} to 10 h^{-1}) and methanol to water ratio (30/70 to 40/60). Pure methanol feed in the flow reaction system enhances the alkane yields considerably, as shown in table 2.

In-situ FT-IR experiments show that, initially, all the hydroxyl groups in the catalyst disappear on exposure to methanol gas, as expected from the formation of methoxyl species. However, the hydroxyl groups reappear as the hydrocarbons start to form. But no aromatics are visible, and this eliminates the possibility that their absence is attributable to the insensitivity of the gas chromatographic method.

Differences in product distribution between the static reaction system and the flow reaction system can be understood in terms of the product sequence that has

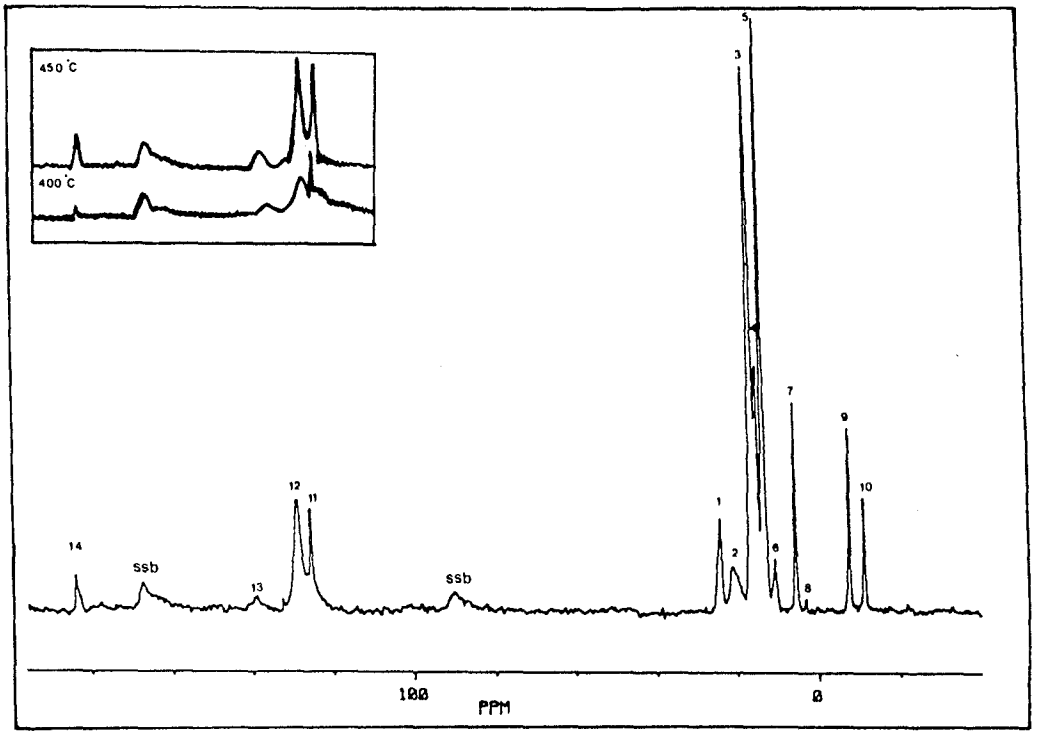

Fig. 3. ^{13}C spectra recorded after heat-treatment at 450 °C for 20 min. and acquired with high-power decoupling. The paraffins produced are similar to those of the previous spectrum but varying dramatically in composition. Methane (9.10); ethane (7, 8); propane (3, 4); butanes (1, 5); benzene (12); methyl-benzenes (2, 13); CO_2 (11); CO (14). The inset shows that the relative amounts of aromatics change as a function of temperature.

already been proposed for ZSM-5 [12,13], in which methanol is converted successfully into DME, alkenes, alkanes and, finally aromatics.

Ethene is the first olefin postulated in this suggested reaction pathway [12]. In support of this suggestion, we have found that the product distribution obtained from a H-SAPO-34 catalyst, when ^{13}C-labeled ethene is adsorbed and heated at 250 °C, is very similar to that reported above (fig. 4).

High olefin selectivity obtained from the flow reaction system, we believe, is the consequence of the short residence times. Continuous flushing of the reaction system removes the olefins as soon as they are produced, thereby arresting their further conversion. Maximum selectivity of olefins can be obtained only in a certain range of flow rate which is the result of optimised reaction rates of different intermediates. The pure paraffins obtained in the static systems stems from the longer residence times. The olefins are produced first and then converted into paraffins under equilibrium reaction conditions. The source of the hydrogen that is required for this conversion is unclear, but it could be the result of a disproportionation reaction, which also yields coke.

Table 1
Product distribution in the flow reaction system, with a 40/60 methanol/water feed, detected by GC and in the static reaction system monitored by ^{13}C MAS NMR. s: strong, s^+: stronger than s, s^{++}: much stronger, m: medium, m^+: stronger than m, w: weak, vw: very weak, *: negligible, –: not observed

Product distribution	Reaction conditions							
	Static reaction system (^{13}C-MAS-NMR)				Flow reaction system (Gas chromatography)			
	300 °C 20 min	350 °C 10 min	400 °C 10 min	400 °C 20 min	300 °C 20 min	350 °C 10 min	400 °C 10 min	400 °C 20 min
CH_4	–	m	m^+	m^+	1.2	1.4	1.1	1.1
C_2H_4	–	–	–	–	15.0	22.7	30.3	33.1
C_2H_6	vw	m	m^+	m^+	*	*	*	*
C_3H_6	–	–	–	–	13.6	20.0	27.0	29.1
C_3H_8	s	s^+	s^{++}	s^{++}	*	*	*	*
C_4H_8	–	–	–	–	5.7	9.4	11.8	13.2
C_4H_{10}	s	s^+	s^{++}	s^{++}	*	*	*	*
C_5H_{12}	w	w	–	–	*	*	*	*
C_6H_{14}	vw	vw	–	–	–	–	–	–
Benzene	–	–	w	m	–	–	–	–
methyl benzenes	–	–	w	m	–	–	–	–

The involvement of water in the flow reaction system causes higher olefin yields as a result of the competition for the Bronsted acid sites between the different basic species. Water, compared with methanol and olefins, is the strongest base and is more likely to occupy the strongest acid sites with fewer and weaker acid sites left in the catalyst. The optimum ratio of water is a function of the hydrothermal stability of the structure and the conversion rate of olefins.

The appearance of aromatics in the static system stems from a combination of appropriate acidity of th catalyst and longer residence times. The conversion of alkanes to aromatics requires overcoming a high energy barrier. The medium acidity of H-SAPO-34 makes the reaction thermodynamically possible and at the same time kinetically slow. Long residence times of alkanes on H-SAPO-34 lead to their final conversion to aromatics. An increase in residence times and reaction

Table 2
Product distribution at 400 °C in the flow reaction system with 40/60 and 100/0 methanol to water feeds, respectively (detected by GC)

$MeOH/H_2O$	Products						
	C_2H_4	C_2H_6	C_3H_6	C_3H_8	C_4H_8	C_4H_{10}	$> C_5$
40/60	33.1	*	29.1	*	13.2	*	*
100/0	20.4	8.8	19.5	14.5	6.5	7.2	*

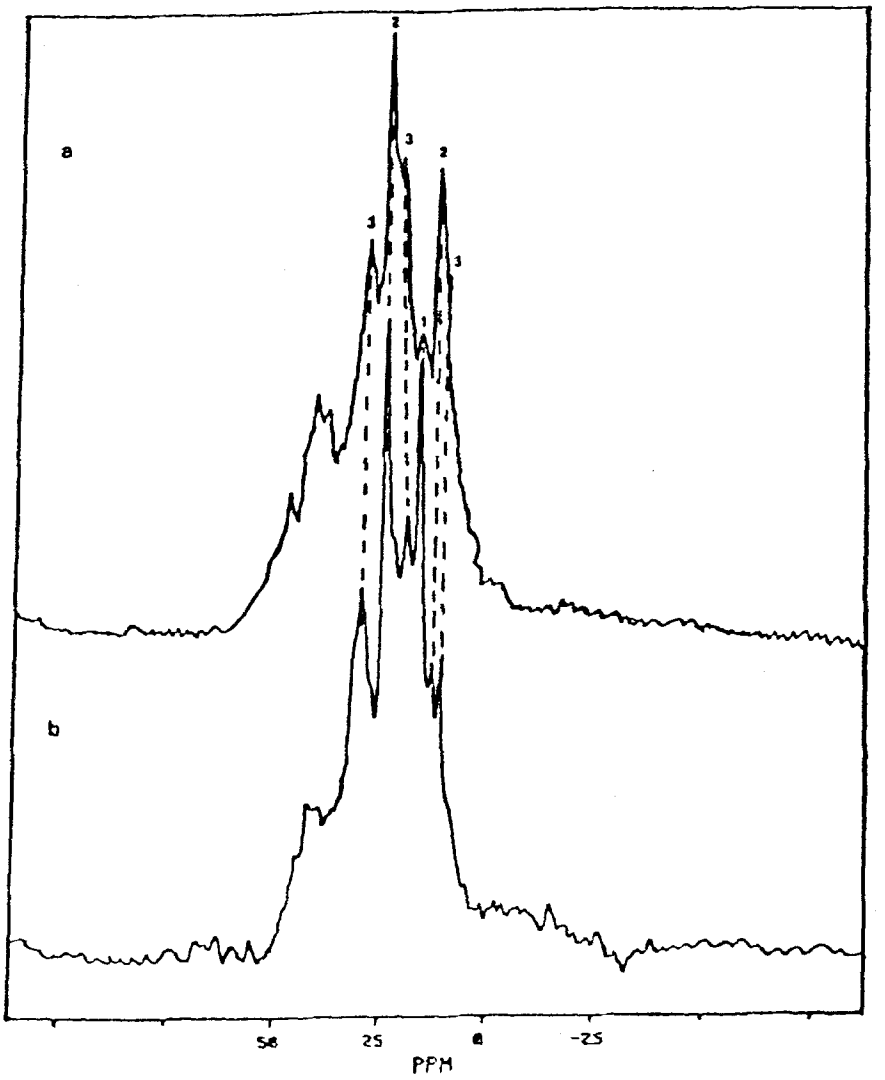

Fig. 4. ^{13}C spectra recorded after heat-treatment and acquired with CP. (a. static conversion of ethene over H-SAPO-34 at 250 °C for 2 min; b. static conversion of methanol over H-SAPO-34 at 350 °C for 10 min.) Propane (1); butane (2), *iso*-pentane (3).

temperatures result in a high proportion of aromatics as shown in fig. 3. In comparison, the high yield of aromatics in the H-ZSM-5 catalytic reaction system (both flow and static) [8] is due to the much stronger acidity of H-ZSM-5 and the large pore dimension. The medium acidity of H-SAPO-34 and its small pore size allow for methanol to be converted, as observed in the flow system, with a high olefin selectivity and without the formation of aromatics. The pore size of a catalyst plays an important role in controlling the product distribution. This may be due to the limiting product diffusion rate which leads to a perturbation of the

reaction equilibrium as in H-ZSM-5 for aromatics [8]. We believe that this is not the case in H-SAPO-34. The acidity of H-SAPO-34 is a more important factor in deciding the product distribution, while the effect of its structure on the product selectivity is of less importance.

The decrease in the concentration of larger than C_4 paraffins in the static system above 400 °C is thought to result from their conversion into aromatics in dehydrogenation and disproportionation reactions. The increase of ethane above 450 °C may be a side product in the sequence of the formation of aromatics.

4. Conclusions

Hydrocarbon formation from methanol on H-SAPO-34 has been investigated in a closed static system by ^{13}C MAS NMR and in an open flow system by gas chromatography. Methanol is shown to be converted via the same pathway in either the static or the flow systems but with steady state and non-steady state modes respectively. High olefin selectivity and negligible amounts of liquid products may be obtained in this particular case by appropriate adjustment of the experimental conditions. The medium acidity of H-SAPO-34 is thought to be a determinant of its good selectivity towards the production of light olefins.

Acknowledgements

We thank the British Council, the Chinese Government and S.E.R.C. for supporting this work. Drs. C.M. Dobson, I.E. Maxwell and A.K. Nowak contributed to many helpful discussions, and Mr. D. Madill produced valuable technical assistance.

References

[1] C.D. Chang, Catal. Rev.-Sci. Eng. 25 (1983) 1.
[2] W.O. Haag and D.H. Olson, U.S. Patent 4, 097, 543 (1978).
[3] E.G. Derouane, J.B. Nagy, P. Dejaifve, J.H.C. van Hooff, B.P. Spekman, J.C. Vedrine and C. Naccache, J. Catal. 53 (1978) 40.
[4] S. Cartlidge and R. Patel, *Proc. 8th Int. Conf. Zeolites* (Elsevier, Amsterdam, 1989) p. 1151.
[5] L. Juan, S.Q. Zhao, H.Y. Li, W.G. Guo and M.L. Ying, *Intl. Symp. Zeolites as catalysts, sorbents and detergent builders* (Wurzburg, 1988) p. 59.
[6] J.M. Thomas, C.A. Fyfe, S. Ramdas, J. Klinowski, G.C. Gobbi and M.W. Anderson, *Intrazeolite Chemistry* (ACS Symposium Series, 218, 1983), p. 159.
[7] T.A. Carpenter, J. Klinowski, D.T.B. Tennakoon, C.J. Smith and D.C. Edwards, J. Magn. Reson. 68 (1986) 561.
[8] M.W. Anderson and J. Klinowski, Nature 339 (1989) 200.

[9] Y. Xu, P.J. Maddox and J.W. Couves, J. Chem. Soc. Faraday Trans. 1, 86 (1990).
[10] W.L.O. Earl and D.L. Vanderhart, J. Mag. Reson. 48 (1982) 35.
[11] C.J.G. Van der Grift, J.W. Geus, M.J. Kappers and J.H. van der Maas, Cat. Lett. 3 (1989) 159.
[12] E.G. Derouane, J.P. Gilson and J.B. Nagy, J. Mol. Catal. 10 (1981) 331
[13] S.L. Meisel, Phil. Trans. Roy. Soc. (London), A300 (1981) 157.